Dynamical theory of single-photon transport in a one-dimensional waveguide coupled to identical and nonidentical emitters

Zeyang Liao,[1,*] Hyunchul Nha,[2] and M. Suhail Zubairy[1]
[1]*Institute for Quantum Science and Engineering (IQSE) and Department of Physics and Astronomy, Texas A&M University, College Station, Texas 77843-4242, USA*
[2]*Department of Physics, Texas A&M University at Qatar, Education City, P.O. Box 23874, Doha, Qatar*
(Received 30 August 2016; published 21 November 2016)

We develop a general dynamical theory for studying a single-photon transport in a one-dimensional (1D) waveguide coupled to multiple emitters which can be either identical or nonidentical. In this theory, both the effects of the waveguide and non-waveguide vacuum modes are included. This theory enables us to investigate the propagation of an emitter excitation or an arbitrary single-photon pulse along an array of emitters coupled to a 1D waveguide. The dipole-dipole interaction induced by the non-waveguide modes, which is usually neglected in the literature, can significantly modify the dynamics of the emitter system as well as the characteristics of the output field if the emitter separation is much smaller than the resonance wavelength. Nonidentical emitters can also strongly couple to each other if their energy difference is less than or of the order of the dipole-dipole energy shift. Interestingly, if their energy difference is close but nonzero, a very narrow transparency window around the resonance frequency can appear which does not occur for identical emitters. This phenomenon may find important applications in quantum waveguide devices such as optical switches and ultranarrow single-photon frequency comb generator.

DOI: 10.1103/PhysRevA.94.053842

I. INTRODUCTION

Photonic structure with reduced dimensions, such as one-dimensional (1D) photonic waveguides, cannot only enhance the photon-emitter interaction but also guide photons, which may find important applications in quantum devices and quantum information [1,2]. A number of systems can be treated as a 1D waveguide such as optical nanofibers [3], photonic crystals with line defects [4], surface-plasmon nanowires [5], and superconducting microwave transmission lines [6–10]. These 1D systems are also excellent platforms for studying many-body physics since the interaction between the emitters induced by the waveguide modes can be long range [11]. Strong photon-photon interactions may be also achieved in these systems [12–16]. In analogy with "cavity quantum electrodynamics (QED)," this system is usually termed as "waveguide QED" [17].

The stationary results of the photon transport in a waveguide-QED system, including a single photon or multiple photons interacting with a single emitter or multiple emitters, have been extensively studied based on the Bethe-ansatz approach [18–23], Lippmann–Schwinger scattering theory [24,25], input-output theory [26–28], the Lehmann–Symanzik–Zimmermann reduction approach [29], and the diagrammatic method [30,31]. In addition, dynamical theories, which allow us to study the real-time evolution of the emitter excitations and photon pulse, have also been studied [32–36]. Many applications of the waveguide-QED system have been proposed, such as highly reflecting mirrors [37–39], single-photon diodes [40–42], efficient single-photon frequency converters [43–46], single-photon transistors [47–51], photonic quantum gates [52–54], and single-photon frequency comb generator [55].

In the previous calculations [17–22,24–30,32–36], the effect of the non-waveguide vacuum modes is included by simply adding a phenomenological decay factor in the Hamiltonian. This approximation is valid when the emitter separation is of the order of or larger than the resonant wavelength. However, it was recently shown that cold atoms can be trapped around a 1D waveguide even in the subwavelength region [56–58]. Quantum dots array with subwavelength separation can be also engineered [59]. If the emitter separation is much smaller than the resonance wavelength, the emitter dipole-dipole interaction induced by the non-waveguide vacuum modes cannot be neglected [60–63]. In addition, the emitters may have different transition frequencies due to the inhomogeneous local fields or nonuniform impurities [64], which is seldom considered in this system.

In this paper, going beyond earlier works, we develop a dynamical theory for single-photon transport in a 1D waveguide-QED system where the emitters can be either identical or nonidentical and both the effects of the waveguide and the non-waveguide vacuum modes are included. When the emitter separation is much smaller than the resonant wavelength, the emitter dynamics and emission spectra can be significantly modified by the dipole-dipole interaction induced by the non-waveguide vacuum modes. From the modifications of the reflection and transmission spectra, we can clearly compare the results with and without the dipole-dipole interaction induced by the non-waveguide vacuum modes. We find that the dipole-dipole interaction induced by the non-waveguide vacuum modes can induce photon transparency in the waveguide system. In addition, we also show that emitters with different transition frequencies can also significantly couple to each other and induce remarkable coherence effects. From the emission spectra we can quantify the effects of the dipole-dipole interaction between emitters with different transition frequencies, and we show the transition from coupled emitters to independent emitters as their energy difference increases.

*zeyangliao@physics.tamu.edu

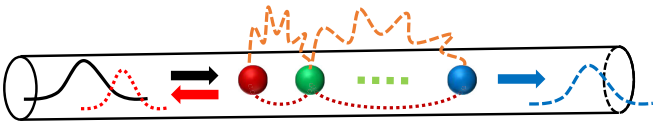

FIG. 1. Single-photon transport in a 1D waveguide coupled to multiple identical or nonidentical emitters. The emitters can couple to each other via the waveguide and non-waveguide photon modes. Black solid curve is the incident field, red dotted curve is the reflected field, and blue dashed curve is the transmitted field.

Interestingly, when the energy difference between the emitters is close but nonzero, a very narrow transparency window can occur around the resonance frequency. A similar effect has been studied in an ensemble of atoms based on semiclassical and mean-field theory and is named dipole-dipole induced electromagnetic transparency (DIET) [65]. Here, we provide an *ab initio* calculation for the DIET and this phenomenon may be easier to experimentally observe in our system. Our theory here may provide an important tool for studying many-body physics and designing new waveguide-based quantum devices.

This paper is organized as follows: In Sec. II, we derive dynamical equations for single-photon transport in a 1D waveguide coupled to identical or nonidentical emitters including the effects of the non-waveguide photon modes. We also derive the reflection and transmission photon spectra of this system. In Sec. III, we compare the results with and without including the dipole-dipole interaction induced by the non-waveguide photon modes in the cases that one emitter is initially excited or a one single-photon pulse is incident. By calculating the emission-spectrum difference, we quantify the effects of the dipole-dipole interaction induced by the non-waveguide photon modes. In Sec. IV, we study the photon transport in the case of nonidentical emitters where we show that DIET can occur in this system. We also show the transition from coupled emitters to independent emitters by increasing the emitter energy difference. In Sec. V, we study the results beyond the two-emitter system where we show that very narrow single-photon frequency combs can be generated. Finally, we summarize our results.

II. MODEL AND THEORY

A. Emitter excitation dynamics

We consider a single-photon transport in a 1D waveguide coupled to multiple quantum emitters which may have different transition frequencies (Fig. 1). The emitters can interact with the waveguide and non-waveguide photon modes. The interaction Hamiltonian in the rotating wave approximation is given by [66]

$$H = \hbar\sum_{j=1}^{N_a}\sum_{k}\left(g_k^j e^{ikz_j}\sigma_j^+ a_k e^{-i\delta\omega_k^j t} + \text{H.c.}\right) + \hbar\sum_{j=1}^{N_a}\sum_{\vec{q}_\lambda}\left(g_{\vec{q}_\lambda}^j e^{i\vec{q}\cdot\vec{r}_j} a_{\vec{q}_\lambda}\sigma_j^+ e^{-i\delta\omega_{\vec{q}_\lambda}^j t} + \text{H.c.}\right), \quad (1)$$

where the first term is the coupling between the quantum emitters and the waveguide photon modes, and the second term is the coupling between the quantum emitters and the non-waveguide photon modes. Here, N_a is the number of quantum emitters, $\delta\omega_k^j = \omega_k - \omega_j$ ($\delta\omega_{\vec{q}_\lambda} = \omega_{\vec{q}_\lambda} - \omega_j$) is the detuning between the transition frequency of the jth emitter ω_j and the frequency ω_k ($\omega_{\vec{q}_\lambda}$) of the guided photon with wave vector k (non-waveguide photon modes with polarization λ and wave vector $\vec{q}$). If ω_j is far away from the cutoff frequency of the photonic waveguide and the waveguide photon has a narrow bandwidth, we can linearize the waveguide photon dispersion relation as $\delta\omega_k^j = (|k| - k_j)v_g$ where k_j is the wave vector at frequency ω_j and v_g is the group velocity [67]. $\sigma_j^+ = |e\rangle_j\langle g|$ ($\sigma_j^- = |g\rangle_j\langle e|$) is the raising (lowering) operator of the jth emitter with position r_j (z_j is its z component along the waveguide direction). $a_k^\dagger$ (a_k^-) and $a_{\lambda,\vec{q}}^\dagger$ ($a_{\lambda,\vec{q}}^-$) are the creation (annihilation) operators of a guided photon and a non-guided photon. $g_k^j = \vec{\mu}_j\cdot\vec{E}_k(\vec{r}_j)/\hbar$ is the coupling strength between the jth emitters and the guided photon modes, with $\vec{\mu}_j$ being the transition dipole moment of the jth emitter and $\hbar$ being Planck's constant, and $g_{\lambda,\vec{q}}^j = \vec{\mu}_j\cdot\vec{E}_{\lambda,\vec{q}}(\vec{r}_j)/\hbar$ is the coupling strength between the jth quantum emitter and the non-guided photon modes.

For a single-photon excitation, the quantum state of the system at an arbitrary time can be expressed as

$$|\Psi(t)\rangle = \sum_{j=1}^{N_a}\alpha_j(t)|e_j,0_k,0_{\vec{q}_\lambda}\rangle + \sum_k\beta_k(t)|g,1_k,0_{\vec{q}_\lambda}\rangle + \sum_{\vec{q}_\lambda}\gamma_{\vec{q}_\lambda}(t)|g,0_k,1_{\vec{q}_\lambda}\rangle, \quad (2)$$

where $|e_j,0_k,0_{\lambda,\vec{q}}\rangle$ is the state in which only the jth emitter is excited with zero waveguide and non-waveguide photons, $|g,1_k,0_{\lambda,\vec{q}}\rangle$ is the state in which all the emitters are in the ground state and one waveguide photon is generated with zero non-waveguide photons, and $|g,0_k,1_{\vec{q}_\lambda}\rangle$ is the state where all the emitters are in the ground state and one non-waveguide photon is generated with zero photons being in the waveguide. $\alpha_j(t)$, $\beta_k(t)$, and $\gamma_{\vec{q}_\lambda}(t)$ are the corresponding amplitudes at time t.

From the Schrödinger equation $i\hbar\partial_t|\Psi(t)\rangle = H|\Psi(t)\rangle$ with Hamiltonian given by Eq. (1) and the quantum state given by Eq. (2), we obtain the following dynamical equations for the probability amplitudes:

$$i\dot{\alpha}_j(t) = \sum_k g_k^j e^{ikz_j - i\delta\omega_k^j t}\beta_k(t) + \sum_{\vec{q}_\lambda} g_{\vec{q}_\lambda}^j e^{i\vec{q}\cdot\vec{r}_j - i\delta\omega_{\vec{q}_\lambda}^j t}\gamma_{\vec{q}_\lambda}(t), \quad (3)$$

$$i\dot{\beta}_k(t) = \sum_{j=1}^{N_a} g_k^{j*} e^{-ikz_j} e^{i\delta\omega_k^j t}\alpha_j(t), \quad (4)$$

$$i\dot{\gamma}_{\vec{q}_\lambda}(t) = \sum_{j=1}^{N_a} g_{\vec{q}_\lambda}^{j*} e^{-i\vec{q}\cdot\vec{r}_j} e^{i\delta\omega_{\vec{q}_\lambda}^j t}\alpha_j(t). \quad (5)$$

Integrating Eqs. (4) and (5), we obtain the formal solutions of the photon amplitudes which are given

by

$$\beta_k(t) = \beta_k(0) - i\sum_{j=1}^{N_a} g_k^{j*} e^{-ikz_j} \int_0^t \alpha_j(t') e^{i\delta\omega_k^j t'} dt', \quad (6)$$

$$\gamma_{\vec{q}_\lambda}(t) = \gamma_{\vec{q}_\lambda}(0) - i\sum_{j=1}^{N_a} g_{\vec{q}_\lambda}^{j*} e^{-i\vec{q}\cdot\vec{r}_j} \int_0^t \alpha_j(t') e^{i\delta\omega_{\vec{q}_\lambda}^j t'} dt', \quad (7)$$

where $\beta_k(0)$ is the initial guided-photon amplitude, and $\gamma_{\vec{q}_\lambda}(0)$ is the initial non-guided-photon amplitude. In this paper, we assume that there is no photon in the non-waveguide photon modes initially, i.e., $\gamma_{\vec{q}_\lambda}(0) = 0$. Inserting Eqs. (6) and (7) into Eq. (3), we obtain

$$\begin{aligned}\dot{\alpha}_j(t) = &- i\sum_k g_k^j e^{ikz_j} e^{-i\delta\omega_k^j t}\beta_k(0) \\ &- \sum_{l=1}^{N_a}\sum_k g_k^j g_k^{l*} e^{ik(z_j - z_l)} \int_0^t dt' \alpha_l(t') e^{i\delta\omega_k^l t'} e^{-i\delta\omega_k^j t} \\ &- \sum_{l=1}^{N_a}\sum_{\vec{q},\lambda} g_{\vec{q}_\lambda}^j g_{\vec{q}_\lambda}^{l*} e^{i\vec{q}\cdot(\vec{r}_j - \vec{r}_l)} \int_0^t dt' \alpha_l(t') e^{i\delta\omega_{\vec{q}_\lambda}^l t'} e^{-i\delta\omega_{\vec{q}_\lambda}^j t},\end{aligned} \quad (8)$$

where the first term is the excitation by the incident waveguide photon, the second and third terms are the coupling between the emitters induced by the waveguide vacuum modes and non-waveguide vacuum modes, respectively.

By summing over the second and third terms of Eq. (8) using the Weisskopf–Wigner approximation, we can obtain closed dynamical evolution equations of the emitters given by (see appendix)

$$\dot{\alpha}_j(t) = b_j(t) - \sum_{l=1}^{N_a}\left[V_{jl}^{(w)} e^{ik_l z_{jl}} \alpha_l\left(t - \frac{z_{jl}}{v_g}\right)\right. \quad (9)$$

$$\left. + V_{jl}^{(nw)} e^{ik_l r_{jl}} \alpha_l\left(t - \frac{r_{jl}}{v_g}\right)\right] e^{i\Delta\omega_{jl} t}, \quad (10)$$

with $j = 1, \ldots, N_a$. In Eq. (9),

$$b_j(t) = \frac{-i}{2\pi}\sqrt{\frac{\Gamma_j v_g L}{2}} e^{ik_a z_j} e^{i\Delta k_j v_g t} \int_{-\infty}^{\infty} \beta_0(\delta k) e^{i\delta k(r_j - v_g t)} d\delta k \quad (11)$$

is the incident photon excitation, $V_{jj}^{(w)} = \Gamma_j/2$ with $\Gamma_j = 2L|g_{k_a}^j|^2/v_g$ being the decay rate of the jth emitter due to the waveguide vacuum modes (L is the quantization length of the waveguide,) and $V_{jj}^{(nw)} = \gamma_j/2$ with $\gamma_j = k_j^3\mu_j^2/3\pi\hbar\epsilon_0 V$ are the spontaneous decay rate of the jth emitter due to the non-waveguide vacuum modes (ϵ_0 is vacuum permittivity and V is the quantization volume). For $j \neq l$, $V_{jl}^{(w)} = \sqrt{\Gamma_j\Gamma_l}/2$ is the dipole-dipole coupling strength due to the waveguide vacuum modes with $z_{jl} = |z_j - z_l|$ and

$$V_{jl}^{(nw)} = \frac{3\sqrt{\gamma_j\gamma_l}}{4}\left[\frac{-i}{k_a r_{jl}} + \frac{1}{(k_a r_{jl})^2} + \frac{i}{(k_a r_{jl})^3}\right] \quad (12)$$

is the dipole-dipole interaction due to the non-waveguide photon modes with $r_{jl} = |\vec{r}_j - \vec{r}_l|$ where we assume the emitter dipole moment is perpendicular to the emitter chain. $\Delta k_j = k_j - k_a$ where k_a can be chosen as the average emitter wave vector. The term $e^{i\Delta\omega_a^{jl} t}$ is due to the energy difference between the jth and lth emitters with $\Delta\omega_{jl} = (k_j - k_l)v_g$. If the emitters have the same transition frequencies, the equation describes the case for identical emitters. By using Eq. (9) and the given initial conditions, we can calculate the real-time evolution of the emitter system with arbitrary configurations.

B. Emission spectra

In addition to the emitter excitation, we can also calculate the emission photon spectrum. The waveguide photon spectrum at arbitrary time can be also calculated by Eq. (6) after obtaining the emitter excitation $\alpha_j(t)$. For simplicity, we assume $\Gamma_j = \Gamma$ and $\gamma_j = \gamma$ in the following calculations. Particularly, long time after the interaction, i.e., $t \to \infty$, the reflection and transmission waveguide photon spectra are given by

$$\beta_R(\delta k) = -i\sqrt{\frac{\Gamma v_g}{2L}}\sum_{j=1}^{N_a} e^{ikz_j} \int_0^{\infty} \alpha_j(t') e^{i(\delta k - \Delta k_j)v_g t'} dt', \quad (13)$$

$$\beta_T(\delta k) = \beta_0(\delta k) - i\sqrt{\frac{\Gamma v_g}{2L}}\sum_{j=1}^{N_a} e^{-ikz_j} \times \int_0^{\infty} \alpha_j(t') e^{i(\delta k - \Delta k_j)v_g t'} dt', \quad (14)$$

where $k = k_a + \delta k$.

We can perform the Fourier transformation and define

$$\chi_j(\delta k) = \int_{-\infty}^{\infty} \alpha_j(t)\Theta(t) e^{i\delta k v_g t} dt, \quad (15)$$

where $\Theta(t)$ is the unit step function with $\Theta(t) = 1$ for $t \geqslant 0$ and $\Theta(t) = 0$ for $t < 0$. The photon spectra shown in Eqs. (12) and (13) can then be rewritten as

$$\beta_R(\delta k) = -i\sqrt{\frac{\Gamma v_g}{2L}}\sum_{j=1}^{N_a} e^{ikz_j}\chi_j(\delta k - \Delta k_j), \quad (16)$$

$$\beta_T(\delta k) = \beta_0(\delta k) - i\sqrt{\frac{\Gamma v_g}{2L}}\sum_{j=1}^{N_a} e^{-ikz_j}\chi_j(\delta k - \Delta k_j). \quad (17)$$

Therefore, to calculate the photon spectrum we need to first calculate $\chi_j(\delta k)$. For this purpose, we perform the inverse Fourier transform

$$\alpha_j(t)\Theta(t) = \frac{v_g}{2\pi}\int_{-\infty}^{\infty} \chi_j(\delta k) e^{-i\delta k v_g t} d\delta k. \quad (18)$$

Next, by using the relation $d/dt[\alpha_j(t)\Theta(t)] = \dot{\alpha}_j(t)\Theta(t) + \alpha_j(0)\delta(t)$, we obtain a set of linear equations for $\chi_j(\delta k)$ from Eq. (9) which are given by

$$\begin{aligned}&-i(\delta k - \Delta k_j)v_g\chi_j(\delta k - \Delta k_j) \\ &\quad = A_j(\delta k - \Delta k_j) - \sum_{l=1}^{N_a} V_{jl} e^{ikz_{jl}}\chi_l(\delta k - \Delta k_l).\end{aligned} \quad (19)$$

Here, for simplicity, we assumed that the emitters are all aligned with the waveguide and we have $r_{jl} = z_{jl}$ and $V_{jl} = V_{jl}^{(w)} + V_{jl}^{(nw)}$. In Eq. (18), $A_j(\delta k) = \alpha_j(0) + b_j(\delta k)$ where $\alpha_j(0)$ is the initial excitation of the jth emitter, and

$$b_j(\delta k) = -i\sqrt{\frac{\Gamma L}{2v_g}}\beta_0(\delta k + \Delta k_j)e^{i(k_j+\delta k)z_j} \tag{20}$$

is the initial waveguide photon spectrum.

The solution of Eq. (18) can be calculated as

$$\chi_j(\delta k - \Delta k_j) = \sum_{l=1}^{N_a}[M(\delta k)]_{jl}^{-1}A_l(\delta k - \Delta k_l), \tag{21}$$

where $M(\delta k)$ is an $N_a \times N_a$ matrix with matrix element given by

$$[M(\delta k)]_{pq} = V_{pq}e^{ikz_{pq}} - i(\delta k - \Delta k_p)v_g\delta_{pq}. \tag{22}$$

From Eqs. (15), (16), and (20), we can calculate the reflection and the transmission spectra. For the case with one emitter excitation but without incident photons, we have the photon spectra to the left ("−") and to the right ("+") given by

$$\beta_{\pm}(\delta k) = -i\sqrt{\frac{\Gamma v_g}{2L}}\sum_{j,l=1}^{N_a}\alpha_l(0)[M(\delta k)]_{jl}^{-1}e^{\mp ikz_j}. \tag{23}$$

For a single incident photon pulse without any initial emitter excitation, we have the reflection and transmission spectra given by

$$\beta_R(\delta k) = -\frac{\Gamma}{2}\beta_0(\delta k)\sum_{j,l=1}^{N_a}[M(\delta k)]_{jl}^{-1}e^{ik(z_j+z_l)}, \tag{24}$$

$$\beta_T(\delta k) = \beta_0(\delta k)\left\{1 - \frac{\Gamma}{2}\sum_{j,l=1}^{N_a}[M(\delta k)]_{jl}^{-1}e^{ik(z_l-z_j)}\right\}. \tag{25}$$

For a single-emitter case, it is readily obtained from Eq. (20) that

$$\chi_1(\delta k) = \frac{\alpha_1(0) + b_1(\delta k)}{V_{11} - i\delta k v_g}, \tag{26}$$

where $V_{11} = (\Gamma + \gamma)/2$. When the emitter is initially excited and there is no input photon, i.e., $\alpha_1(0) = 1$ and $b_1(\delta k) = 0$, the spontaneous emission spectrum has the usual Lorentzian lineshape. For a single-photon input with the emitter being initially in the ground state, i.e., $\alpha_l(0) = 0$ and $b_1(\delta k) \neq 0$, the emission spectrum is a Lorentzian function modulated by the input photon spectrum.

In the following sections, we first study the effects of the dipole-dipole interaction induced by the non-waveguide vacuum modes with the two-emitter example. Then we study the effects of nonidentical emitters with the two-emitter example. Finally we study the case of beyond the two-emitter system.

III. EFFECTS OF DIPOLE-DIPOLE INTERACTION INDUCED BY NON-WAVEGUIDE VACUUM MODES

In this section, we consider the emitters to be identical and compare the results with and without including the dipole-dipole interaction induced by the non-waveguide vacuum mode. For identical emitters, we have $k_j = k_a$ for all emitters.

For a two-emitter system, the evolution of the emitters is given by

$$\dot{\alpha}_1(t) = b_1(t) - V_{11}\alpha_1(t) - V_{12}e^{ik_az_{12}}\alpha_2\left(t - \frac{z_{12}}{v_g}\right), \tag{27}$$

$$\dot{\alpha}_2(t) = b_2(t) - V_{22}\alpha_2(t) - V_{21}e^{ik_az_{12}}\alpha_2\left(t - \frac{z_{12}}{v_g}\right), \tag{28}$$

where $V_{11} = V_{22} = (\Gamma + \gamma)/2$, $V_{12} = V_{21} = V_{12}^{(w)} + V_{12}^{(nw)}$, and $b_{1,2}(t)$ are given by Eq. (10). Due to the dipole-dipole coupling, the one excitation subspace is split into two eigenstates [$|+\rangle = (|eg\rangle + |ge\rangle)/\sqrt{2}$ and $|-\rangle = (|eg\rangle - |ge\rangle)/\sqrt{2}$] with the energy shifts given by $\pm\mathrm{Im}[V_{12}e^{ik_az_{12}}]$ and the decay rates given by $V_{11} \pm \mathrm{Re}[V_{12}e^{ik_ar_{12}}]$. The $M(\delta k)$ matrix for calculating the emission spectra is given by

$$M(\delta k) = \begin{bmatrix} V_{11} - i\delta k v_g & V_{12}e^{ik_az_{12}} \\ V_{21}e^{ik_az_{12}} & V_{22} - i\delta k v_g \end{bmatrix}. \tag{29}$$

A. Emitter excitation propagation

In this section, we consider the propagation of emitter excitation without incident photon pulse. We assume that the emitter on the left is initially in the excited state while the emitter on the right is initially in the ground state, $\alpha_1(0) = 1$, $\alpha_2(0) = b_{1,2}(\delta k) = 0$. In this case, the photon emission spectra to the left and to the right are given by

$$\beta_-(\delta k) = -i\sqrt{\frac{\Gamma v_g}{2L}}e^{ikz_1}\frac{V_{11} - i\delta k v_g - V_{12}e^{2ikz_{12}}}{(V_{11} - i\delta k v_g)^2 - V_{12}^2e^{2ikz_{12}}}, \tag{30}$$

$$\beta_+(\delta k) = -i\sqrt{\frac{\Gamma v_g}{2L}}e^{-ikz_1}\frac{V_{11} - i\delta k v_g - V_{12}}{(V_{11} - i\delta k v_g)^2 - V_{12}^2e^{2ikz_{12}}}, \tag{31}$$

where $k = k_a + \delta k$.

We compare the emitter dynamics and the emission spectra in the cases with and without including the dipole-dipole interaction induced by the non-waveguide vacuum modes ($V_{dd}^{(nw)}$). Here we study the cases of two emitter separations, i.e., $a = 0.5\lambda$ and $a = 0.05\lambda$. The emitter excitations and the emission spectra when $a = 0.5\lambda$ and $\gamma = 0.2\Gamma$ are shown in Figs. 2(a) and 2(b), respectively. In this case, $V_{ii} = 0.6\Gamma$, $V_{12}^{(w)} = 0.5\Gamma$, and $V_{12}^{(nw)} = 0.015\Gamma - 0.043\Gamma i$. Without including $V_{12}^{(nw)}$, $\mathrm{Im}(V_{12}e^{ik_ar_{12}}) = 0$ which gives zero energy shifts for the two eigenstates. The two decay rates are given by 1.1Γ and 0.1Γ corresponding to a superradiant and a subradiant state, respectively. With $V_{12}^{(nw)}$, the energy shifts are given by $\pm 0.043\Gamma$ and the decay rates are given by 1.115Γ and 0.085Γ. The difference between the cases with and without $V_{12}^{(nw)}$ is very small. Indeed, from Figs. 2(a) and 2(b), we see that both the emitter excitations and the photon spectra are almost the same with (solid curves) and without (dotted curves) including $V_{12}^{(nw)}$. The spectra in two directions are the same and they have Lorentzian lineshapes. Hence, when the emitter separation is relatively large, we can safely neglect the effect of $V_{12}^{(nw)}$ [34].

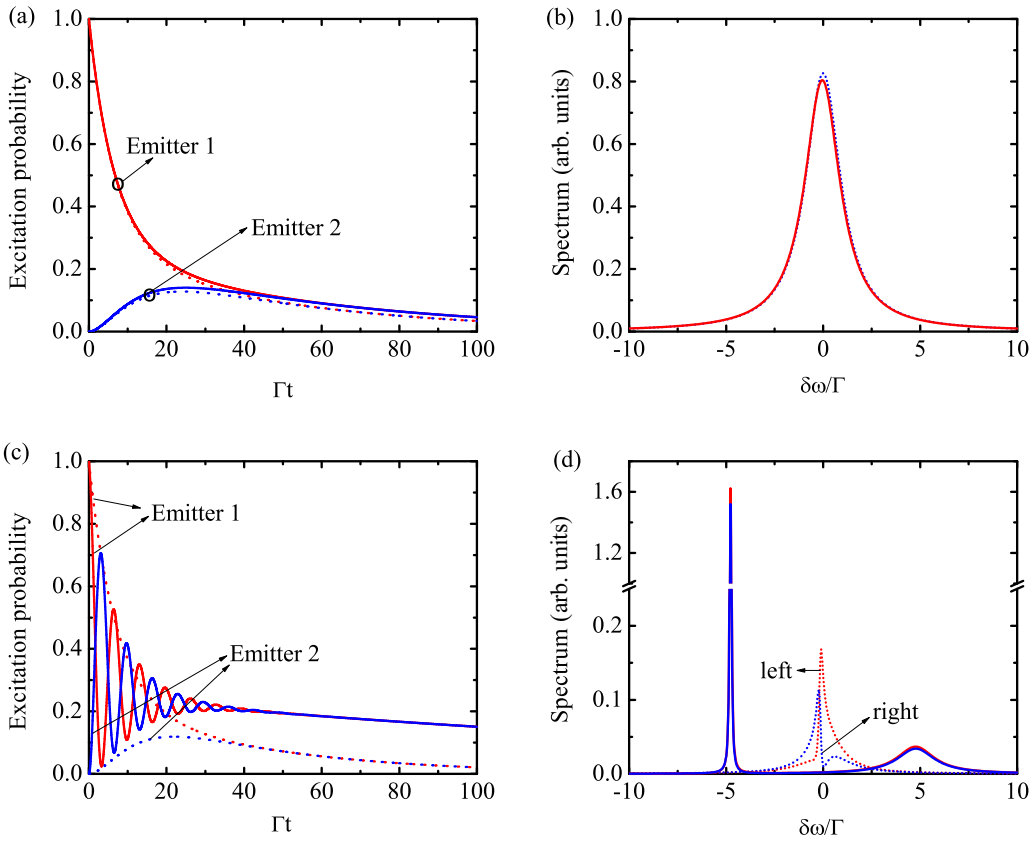

FIG. 2. (a), (c) Emitter excitation dynamics as a function of time. (b), (d) Emission photon spectra. Emitter 1 is initially excited and there is no incident photon. $\alpha_1(0) = 1$, $\alpha_2(0) = b_{1,2}(\delta k) = 0$, $\gamma = 0.2\Gamma$. (a), (b) $a = 0.5\lambda$. (c), (d) $a = 0.05\lambda$. Dotted lines are the results without $V_{12}^{(nw)}$, and the solid curves are the results with $V_{12}^{(nw)}$.

However, when the emitter separation is very small compared with the resonant wavelength, the results are quite different. The emitter excitations and the photon spectra when $a = 0.05\lambda$ with $\gamma = 0.2\Gamma$ are shown in Figs. 2(c) and 2(d), respectively. In this case, $V_{ii} = 0.6\Gamma$, $V_{12}^{(w)} = 0.5\Gamma$, and $V_{12}^{(nw)} = 1.52\Gamma + 4.36\Gamma i$. Without including $V_{12}^{(nw)}$ the energy shifts are $\pm 0.15\Gamma$ and the decay rates are given by 1.08Γ and 0.12Γ. With $V_{12}^{(nw)}$, the energy shifts are $\pm 4.77\Gamma$ and the decay rates are given by 1.17Γ and 0.03Γ. There are large differences due to $V_{12}^{(nw)}$ which can also be seen from Figs. 2(c) and 2(d). Without including $V_{12}^{(nw)}$, the emitter excitation dynamics are similar to the case when $a = 0.5\lambda$. However, with the effect of $V_{12}^{(nw)}$ the two emitters exchange energy many times until they have the same excitation probability and then decay slowly to the ground state. Since the decay rate of the subradiant eigenstate with $V_{12}^{(nw)}$ (0.03Γ) is smaller than that without $V_{12}^{(nw)}$ (0.12Γ), the emitter excitations last much longer with $V_{12}^{(nw)}$ than those without $V_{12}^{(nw)}$. The spectra are also quite different. Without including V_{12}^{nw}, the emission spectra are peaked close to the resonance frequency with Fano-like lineshapes [68,69]. With V_{12}^{nw}, the emission spectra are far away from the resonance frequency. The spectra of the left-moving and the right-moving fields are almost the same with one superradiant peak and one subradiant peak. Therefore, $V_{12}^{(nw)}$ can be a crucial factor to determine the characteristics of the waveguide system if the emission to the non-waveguide modes γ is not too small and the emitter separation is much smaller than the resonance wavelength.

B. Single-photon transport

Next, we consider the case when both emitters are initially in the ground state and there is a single incident photon pulse. The emitter dynamics are given by Eqs. (26) and (27). The reflection and transmission photon spectra are given by

$$\beta_R(\delta k) = -\frac{\Gamma}{2} e^{2ikz_1} \beta_0(\delta k) \times \frac{(V_{11} - i\delta k v_g)(1 + e^{2ikz_{12}}) - 2V_{12}e^{2ikz_{12}}}{(V_{11} - i\delta k v_g)^2 - V_{12}^2 e^{2ikz_{12}}}, \quad (32)$$

$$\beta_T(\delta k) = \beta_0(\delta k)\left[1 - \frac{\Gamma}{2}\frac{2(V_{11} - i\delta k v_g) - V_{12}(1 + e^{2ikz_{12}})}{(V_{11} - i\delta k v_g)^2 - V_{12}^2 e^{2ikz_{12}}}\right], \quad (33)$$

where $k = k_a + \delta k$. If the waveguide is so good that the non-waveguide modes are inhibited (i.e., $\gamma = 0$), we have $V_{ii} = V_{ij} = \Gamma/2$ with $i, j = 1,2$. In this case, it is not difficult to see that for resonance frequency we have $\beta_R(0) = -e^{2ikz_1}\beta_0(\delta k)$ and $\beta_T(0) = 0$. Thus, without non-waveguide vacuum modes, the resonance frequency is completely reflected with a π phase shift [34].

For illustration with the numerical examples, we assume that the photon pulse has a Gaussian shape with a spectrum

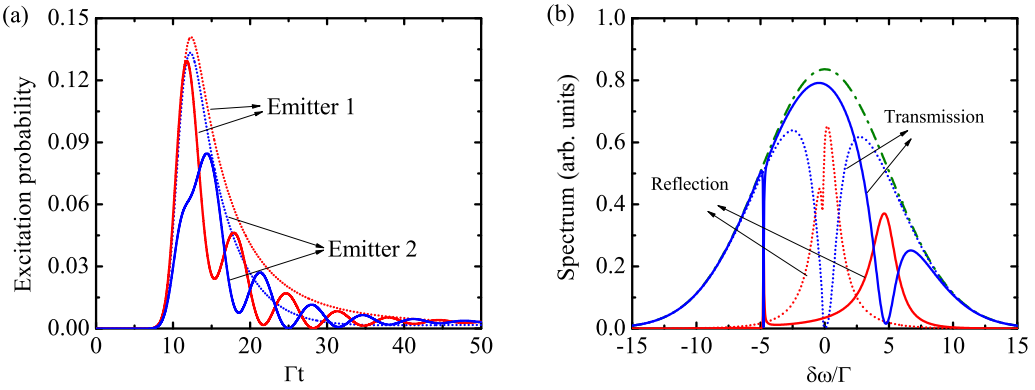

FIG. 3. (a) Emitter excitation probabilities as a function of time excited by an incident photon pulse with (solid lines) and without (dotted lines) $V_{12}^{(nw)}$. (b) Emission photon spectra with and without $V_{12}^{(nw)}$. The green dashed-dotted lines are the incident photon spectrum, the solid curves are the results with $V_{12}^{(nw)}$, and the dotted curves are the results without $V_{12}^{(nw)}$. The parameters are as follows: $\alpha_1(0) = \alpha_2(0) = 0$, $\gamma = 0.2\Gamma$, $\Delta_0 v_g = 10\Gamma$, $z_1 = 10/\Gamma$, and $a = 0.05\lambda$.

given by

$$\beta_0(\delta k) = \frac{(8\pi)^{1/4}}{\sqrt{\Delta_0 L}} e^{-\frac{\delta k^2}{\Delta_0^2}}, \tag{34}$$

where Δ_0 is the width in k space with the full width at half maximum of the spectrum being $\sqrt{2\ln 2}\Delta_0 v_g$. The single-photon condition requires that $(L/2\pi)\int_{-\infty}^{\infty} |\beta_0(\delta k)|^2 d\delta k = 1$. With this Gaussian photon pulse, we have

$$b_j(t) = -i(8\pi)^{-1/4}\sqrt{\Gamma\Delta_0 v_g} e^{ik_0 z_j} e^{-\frac{1}{4}\Delta_0^2 (z_j - v_g t)^2} \tag{35}$$

in Eq. (9). The emitter excitation as a function of time when $a = 0.05\lambda$, $\gamma = 0.2\Gamma$ is shown in Fig. 3(a) where we assume that $\Delta_0 = 10\Gamma$. The two dotted curves are the two-emitter excitations without including $V_{12}^{(nw)}$ and the two solid curves are those with $V_{12}^{(nw)}$. We can see that, without $V_{12}^{(nw)}$, the two emitters are first exited and then deexcited with almost the same excitation dynamics. However, with $V_{12}^{(nw)}$ the excitations of the two emitters can oscillate coherently after being excited by the photon pulse due to the strong dipole-dipole interaction between the two emitters. The emission spectra with and without $V_{12}^{(nw)}$ are also quite different, as shown in Fig. 3(b). In the figure, the two dotted curves are the reflection and transmission spectra without $V_{12}^{(nw)}$ while the solid curves are those with $V_{12}^{(nw)}$. Without $V_{12}^{(nw)}$, the resonant frequency is significantly reflected with negligible transmission. However, with $V_{12}^{(nw)}$, the resonant frequency can almost transmit with two reflection peaks far away from the resonant frequency. This is the phenomenon of dipole-dipole-induced electromagnetic transparency (DIET). Compared to the usual electromagnetic-induced transparency (EIT), where the transparency is caused by a strong pumping field [70], here the transparency is induced by the strong dipole-dipole interaction between the emitters. The strong dipole-dipole interaction can significantly shift the eigenenergy of the system and therefore the resonance frequency can be transmitted. This phenomenon may be used as optical switch [47–49]. By controlling the emitter separation, we can control the dipole-dipole interaction between the emitters to control the transmission of the photons. However, in practice it is not easy to tune the emitter separation. In Sec. IV A, we show that DIET can be achieved by simply tuning the emitter transition frequency which should be more convenient. The reflection occurs at the frequencies far away from the resonant frequency with one peak being the superradiant peak while the other being the subradiant peak similar to Fig. 2(d). This example again shows that, for small emitter separation, the dipole-dipole interaction induced by the non-waveguide vacuum modes can play a nontrivial role if γ is not too small compared with Γ.

C. Spectrum difference with and without $V_{dd}^{(nw)}$

In the last two sections, we have seen that the dipole-dipole interaction induced by the non-guide vacuum modes can significantly affect the emitter dynamics and emission spectra when the emitter separation is much smaller than the resonance wavelength. To further quantify the effects of the dipole-dipole interaction induced by the non-guide vacuum modes, we define the normalized spectrum difference with and without $V_{dd}^{(nw)}$ as

$$\Delta_{SD} = \frac{1}{2}\left\{\frac{\sum_k \left|I_R^1(k) - I_R^2(k)\right|}{\sum_k \left[I_R^1(k) + I_R^2(k)\right]} + \frac{\sum_k \left|I_T^1(k) - I_T^2(k)\right|}{\sum_k \left[2 - I_T^1(k) - I_T^2(k)\right]}\right\}, \tag{36}$$

where $I_R^1(k)$ $[I_T^1(k)]$ is the reflection (transmission) spectrum with $V_{dd}^{(nw)}$ and $I_R^2(k)$ $[I_T^2(k)]$ is the reflection (transmission) spectrum without $V_{dd}^{(nw)}$. Since the background transmission is 1, in the second term of Eq. (35) the quantity $1 - I_T^{1,2}(k)$ is used instead of $I_T^{1,2}(k)$ to avoid divergence in the numerator. If the emission spectra with and without $V_{dd}^{(nw)}$ are completely identical, $\Delta_{SD} = 0$. On the contrary, if the emission spectra with and without $V_{dd}^{(nw)}$ are completely different (i.e., have no overlaps), $\Delta_{SD} = 1$. Therefore, the quantity shown in Eq. (35) is a good measure of the spectrum difference with and without $V_{dd}^{(nw)}$.

In Fig. 4, we plot the spectrum difference for different emitter separations with two different γ ($\gamma = 0.1\Gamma$ and $\gamma = 0.5\Gamma$). When the emitter separation r_{12} approaches zero, the spectrum difference Δ_{SD} approaches 1 which means that the

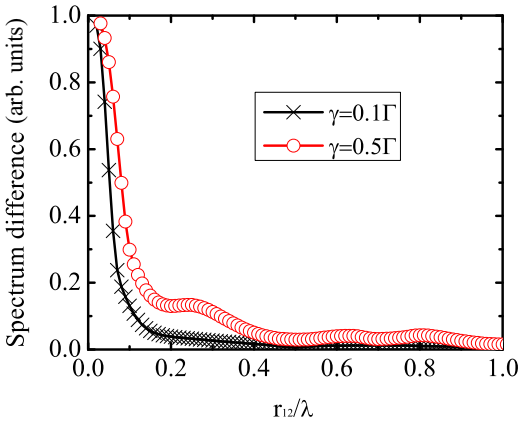

FIG. 4. The normalized spectrum difference between the cases with and without $V_{dd}^{(nw)}$ for different emitter separations. The curve with the cross symbols is the result when $\gamma = 0.1\Gamma$, and the curve with the circle symbols is the result when $\gamma = 0.5\Gamma$.

spectra with and without $V_{dd}^{(nw)}$ for small emitter separation are almost completely different. When the emitter separation r_{12} is of the order of or larger than the resonant wavelength, Δ_{SD} is close to zero which indicates that the spectra with and without $V_{dd}^{(nw)}$ for large emitter separation are almost the same. These observations are consistent with the results shown in previous sections.

For $\gamma = 0.1\Gamma$, the spectrum difference is 0.5 when $r_{12} \simeq 0.05\lambda$. For $\gamma = 0.5\Gamma$, the spectrum difference is 0.5 when $r_{12} \simeq 0.08\lambda$. For both cases, the spectrum difference is 0.5 when $|V_{dd}^{(nw)}| \approx 2\Gamma$. When $|V_{dd}^{(nw)}| \approx 0.2\Gamma$, i.e., $r_{12} \simeq 0.1\lambda$ for $\gamma = 0.1\Gamma$ and $r_{12} \simeq 0.3\lambda$ for $\gamma = 0.5\Gamma$, the spectrum difference is about 10%. Therefore, when $|V_{dd}^{(nw)}| < 0.2\Gamma$, we can safely neglect the effect of $V_{dd}^{(nw)}$. Otherwise, the effect of $V_{dd}^{(nw)}$ should be taken into account.

IV. NONIDENTICAL EMITTERS

In this section, we consider the two-emitter case to illustrate the effects of nonidentical emitters. For this purpose, we let their transition frequencies be different, i.e., $\omega_a^j \neq \omega_a^l$ or $k_j \neq k_l$ if $j \neq l$.

For a two-emitter system, the excitation dynamics of the emitters are given by

$$\dot{\alpha}_1(t) = b_1(t) - V_{11}\alpha_1(t) - V_{12}e^{ik_a r_{12}}e^{i\Delta\omega_{12}t}\alpha_2\left(t - \frac{z_{12}}{v_g}\right), \tag{37}$$

$$\dot{\alpha}_2(t) = b_2(t) - V_{22}\alpha_2(t) - V_{21}e^{ik_a r_{12}}e^{i\Delta\omega_{21}t}\alpha_2\left(t - \frac{z_{12}}{v_g}\right), \tag{38}$$

where $\Delta\omega_{ij} = \omega_i - \omega_j$ with $i, j = 1,2$. The coupling matrix between these two single-emitter excited states reads

$$V(t) = \begin{bmatrix} V_{11} & V_{12}e^{ik_a z_{12}}e^{i\Delta\omega_{12}t} \\ V_{12}e^{ik_a z_{12}}e^{-i\Delta\omega_{12}t} & V_{22} \end{bmatrix}, \tag{39}$$

which is time dependent. It is seen that the coupling between the two emitters is modulated by the energy difference between these two emitters. When $\Delta\omega_{12} = 0$, it reduces to the case of identical emitters. When $\Delta\omega_{12} = \infty$, the rapid oscillations can erase the off-diagonal terms in Eq. (39) and thus eliminate the coupling between the two emitters. The instantaneous single-emitter excited eigenstates are $|\psi_\pm(t)\rangle = (|eg\rangle \pm e^{-i\Delta\omega_{12}t}|ge\rangle)/\sqrt{2}$ and their corresponding eigenvalues are $E_\pm = V_{11} \pm V_{12}e^{ik_a r_{12}}$. Although the eigenvalues are the same as those with identical emitters, the eigenstates here are time dependent, which is quite different from those with identical emitters. Due to the time modulation factor, the two states $|\psi_+\rangle$ and $|\psi_-\rangle$ can interchange with each other as time evolves.

For the two-emitter system, $M(\delta k)$ in Eqs. (23) and (24) is given by

$$M(\delta k) = \begin{bmatrix} V_{11} - i(\delta k - \Delta k_1)v_g & V_{12}e^{ikz_{12}} \\ V_{21}e^{ikz_{12}} & V_{22} - i(\delta k - \Delta k_2)v_g \end{bmatrix}. \tag{40}$$

For a single incident photon pulse, we obtain the reflection and transmission photon spectra given by

$$\beta_R(\delta k) = \frac{\Gamma}{2}e^{2ikr_1}\beta_0(\delta k)\frac{2M_{12}(\delta k)e^{ikz_{12}} - M_{11}(\delta k)e^{2ikz_{12}} - M_{22}(\delta k)}{M_{11}(\delta k)M_{22}(\delta k) - M_{12}^2(\delta k)}, \tag{41}$$

$$\beta_T(\delta k) = \beta_0(\delta k)\left\{1 - \frac{\Gamma}{2}\frac{M_{11}(\delta k) + M_{22}(\delta k) - 2M_{12}(\delta k)\cos(kz_{12})}{M_{11}(\delta k)M_{22}(\delta k) - M_{12}^2(\delta k)}\right\}. \tag{42}$$

It is seen that $\beta_R(\delta k)$ and $\beta_T(\delta k)$ depends on $\beta_0(\delta k)$ but not other frequency components. Therefore, no frequency conversion can occur here.

A. Without non-waveguide modes

In this section, we first consider the case without non-waveguide modes, i.e., $\gamma = 0$. In this case, $V_{11} = V_{22} = V_{12} = \Gamma/2$. Here, we compare the excitation dynamics [Figs. 5(a)–5(c)] and emission photon spectra [Figs. 5(d)–5(f)] when $r_{12} = 0.5\lambda$ for three different emitter energy differences, i.e., $\Delta\omega_{12} = 0$, 0.2Γ, and 2Γ. In these numerical examples, we assume that the input single-photon pulse has a Gaussian shape, as shown in Eq. (33) with $\Delta_0 = \Gamma$. For $r_{12} = 0.5\lambda$, $V_{12}^{(w)}e^{ik_a r_{12}} = -0.5\Gamma$. The energy shift by the dipole-dipole interaction induced by the waveguide photon modes is zero, and the decay rates for the two single-emitter excited eigenstates ($|+\rangle$ and $|-\rangle$) are given by Γ and 0 with one being superradiant and the other being subradiant.

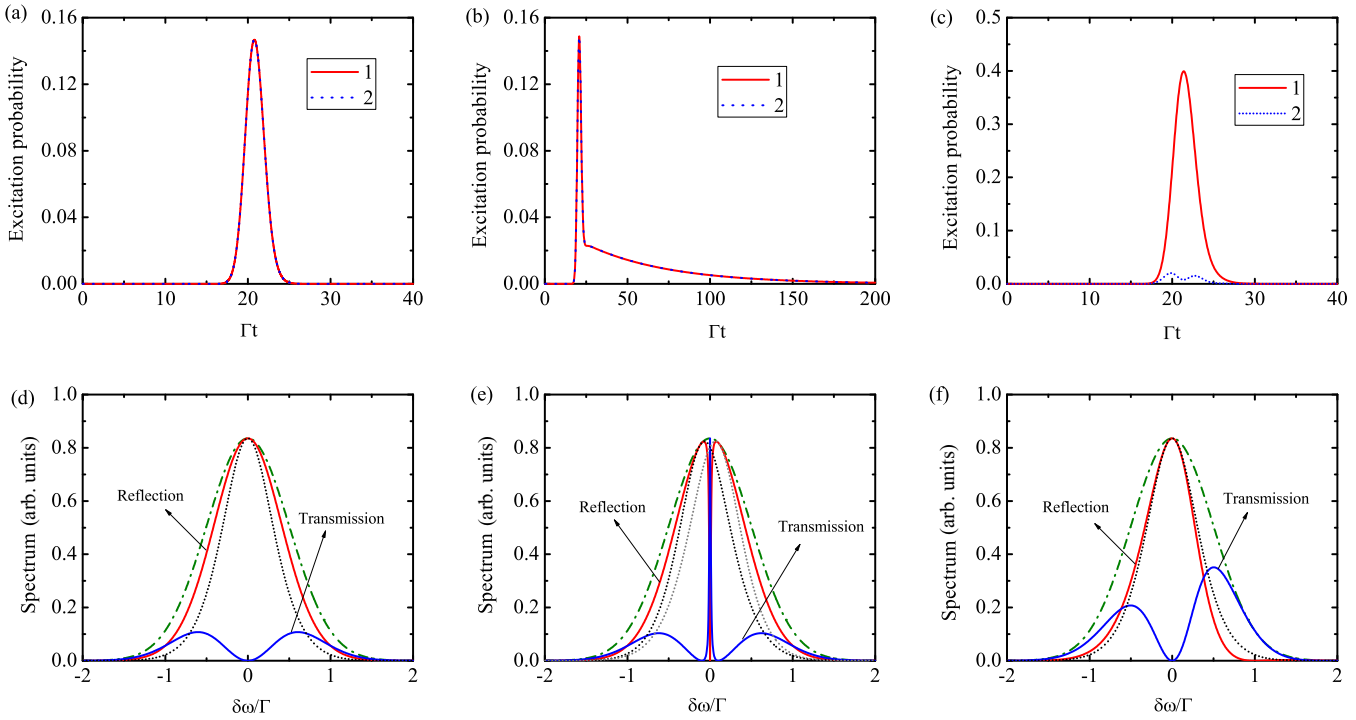

FIG. 5. (a)–(c) Emitter excitation probabilities as a function of time for different emitter energy gaps with single Gaussian photon pulse input. The red solid line is the excitation for emitter 1, and the blue dotted line is the excitation for emitter 2. (d)–(f) Emission spectra for different emitter energy gaps. The green dashed-dotted line is the input photon spectrum, the red and blue solid lines are the reflection and transmission photon spectra of the two-emitter system, and the black and gray dotted lines are the reflection spectrum of the independent emitter case. The parameters are as follows: $\Delta_0 v_g = \Gamma$, $\gamma = 0$, $z_1 = 20/\Delta_0$, $z_{12} = 0.5\lambda$, (a), (d) $\Delta\omega_{12} = 0$, (b), (e) $\Delta\omega_{12} = 0.2\Gamma$, (c), (f) $\Delta\omega_{12} = 2\Gamma$.

When the two emitters are identical ($\Delta\omega_{12} = 0$), both emitters are excited and then deexcited together as the incident pulse propagates through [Fig. 5(a)]. From Eqs. (40) and (41), it is readily seen that $\beta_R(0) = -e^{2ikr_1}\beta_0(\delta k)$ and $\beta_T(0) = 0$, i.e., the resonant frequency is completely reflected. Although the independent-emitter model can also explain the total reflection of the resonance frequency (black dotted line), it cannot explain the broader reflection linewidth for the two-emitter system (red solid line). The broader linewidth is the signature of the superradiant state induced by the collective interaction between the two emitters [Fig. 5(d)].

The results when the two emitters have close but nonzero energy difference (e.g., $\Delta\omega_{12} = 0.2\Gamma$ with $\Delta\omega_a^{(1,2)} = \pm 0.1\Gamma$) are shown in Figs. 5(b) and 5(e). From Fig. 5(b), we see that the two emitters are also excited and then deexcited together. However, different from the case of identical emitters [Fig. 5(a)], the emitter excitations when $\Delta\omega_{12} = 0.2\Gamma$ can last much longer [Fig. 5(b)]. This indicates that the subradiant state can be populated when there is a small energy difference between the two emitters. This can be explained by the fact that the superradiant and subradiant states can interchange with each other when there is a time modulation factor in the coupling matrix, as shown in Eq. (38). In contrast, for two identical emitters, the subradiant state will never be populated when $r_{12} = 0.5\lambda$. The emission photon spectra also become very distinctive [Fig. 5(e)]. Instead of being completely reflected at the resonant frequency as in the identical-emitter case, a very narrow transmission window appears around the resonance frequency when the two emitters have close but nonzero energy difference. This transparency can be seen from Eqs. (40) and (41). For $\delta k r_{12} \ll 1$, we can see from Eq. (40) that when $\delta k v_g = (\Delta\omega_1 + \Delta\omega_2)/2$, we have $\beta_R(0) = 0$ which means the resonance frequency can be completely transparent. However, if we neglect the dipole-dipole coupling between the two emitters ($V_{12} = 0$), we have $|\beta_R(0)/\beta_0(0)| = 1/[1 + (2\Delta\omega_{12}/\Gamma)^2]$ which is close to 1 when $\Delta\omega_{12} \ll \Gamma$. Therefore, the dipole-dipole interaction here is critical for the transmission of the resonance frequency and the phenomena here can also be called dipole-dipole-induced electromagnetic transparency (DIET). Actually, the transparency is the result of destructive interference between two emission channels. DIET has been studied in an atomic ensemble where semiclassical and mean-field theory are applied [65]. Here we provide an *ab initio* calculation for this phenomenon and the system here can be easier to realize in experiment. The DIET here may be used as single-photon switch by tuning the emitter energy.

When the energy difference of the two emitters is large, e.g., 2Γ and one emitter has a transition frequency resonant with the center frequency of the incident photon, we can see that one emitter is excited as a single-emitter case, but the other one is rarely excited by the input photon pulse due to large detuning [Fig. 5(c)]. The emission spectra are also similar to those of the independent-emitter case. Therefore, when the two emitters have a large energy difference (i.e., much greater than their dipole-dipole interaction energy), they behave as independent emitters.

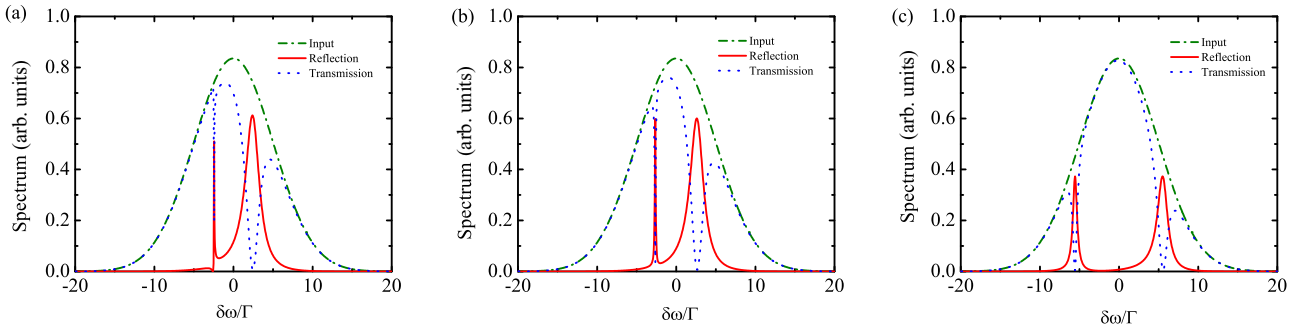

FIG. 6. Emission photon spectrum for different emitter energy gaps including the effects of non-waveguide modes. The green dashed-dotted line is the input photon spectrum, the red (blue) solid lines are the reflection (transmission) photon spectra. The parameters are as follows: $\Delta_0 v_g = 10\Gamma$, $\gamma = 0.1\Gamma$, $z_1 = 20/\Delta_0$, $z_{12} = 0.05\lambda$, (a) $\Delta\omega_{12} = 0$, (b) $\Delta\omega_{12} = 2\Gamma$, (c) $\Delta\omega_{12} = 10\Gamma$.

B. With non-waveguide modes

In this section, we study how the emission spectra change when the emitter energy difference increases in the presence of non-waveguide modes, i.e., $\gamma \neq 0$. The numerical results when $a = 0.05\lambda$ and $\gamma = 0.1\Gamma$ are shown in Fig. 6. In this case, the dipole-dipole interaction is $V_{12}e^{ik_a r_{12}} = 0.52\Gamma + i2.46\Gamma$. The energy shifts due to the dipole-dipole interaction are $\pm 2.46\Gamma$, and the decay rates of the two eigenstates are $\Gamma_+ = 1.07\Gamma$ and $\Gamma_- = 0.03\Gamma$, respectively. In the numerical results, we assume that the incident photon pulse has a Gaussian shape with $\Delta_0 = 10\Gamma$.

The emission spectra when the two emitters are identical are shown in Fig. 6(a). There are two reflection peaks around $\pm 2.46\Gamma$ with one being very broad and the other being very sharp. The peak positions are the same as the energy shifts due to the dipole-dipole interaction. The broad peak has a width of about 2.13Γ which is $2\Gamma_+$ due to the reflection from the superradiant state. The sharp peak has a width of about 0.06Γ which is $2\Gamma_-$ due to the reflection from the subradiant eigenstate.

When the two emitters have different transition frequencies; for example, $\Delta\omega_{12} = 2\Gamma$, there are also two reflection peaks with one being the superradiant peak and the other one being the subradiant peak [Fig. 6(b)]. The positions of the peaks are about $\pm 2.61\Gamma$ which are slightly larger than the energy shifts due to the dipole-dipole interaction. The superradiant peak has a width of about 2.04Γ which is slightly narrower than that of the identical emitters, and the subradiant peak has a width of about 0.12Γ which is slightly broader than that of the identical emitters. Although the difference between these two peaks decreases, the dipole-dipole interaction still plays an important role when the energy difference is of the order of the dipole-dipole-induced energy shift.

If we continue to increase the energy difference such that the energy difference between the two emitters is much larger than the dipole-dipole-induced energy shift; for example, $\Delta\omega_{12} = 10\Gamma$, the emission spectra are quite different from those in Figs. 6(a) and 6(b). The two reflection peaks become more similar to each other with one peak having a width of about 1.56Γ and the other one having a width of about 0.66Γ. The positions of the two peaks are about $\pm 5.5\Gamma$ which is quite different from the energy shifts due to the dipole-dipole interaction. The separation between the two peaks is about 11Γ which is close to the energy difference of the two emitters, which indicates that they behave more like independent emitters.

C. Transition from coupled emitters to independent emitters

In the previous section, we showed that the effective coupling between the emitters depends on the emitter energy difference. In this section, we quantify this dependence by calculating the peak separation and the linewidth difference of the two reflection peaks as a function of emitter energy difference. The peak separation as a function of emitter energy difference when $\gamma = 0.1\Gamma$ and $r_{12} = 0.05\lambda$ are shown in Fig. 7(a). The peak separation increases monotonically as the energy difference increases. When the two emitters are identical, i.e., $\Delta\omega_{12} = 0$, the peak separation is equal to $2\mathrm{Im}(V_{12})$ which means that the two emitters are strongly coupled to each other via the dipole-dipole interaction. However, when the two emitters have a large energy difference, e.g., $\Delta\omega_{12} = 20\Gamma$, the peak separation is close to $\Delta\omega_{12}$ which indicates that the two emitters behave mostly as independent emitters. Thus, the emitters can transit from coupled emitters to independent emitters by increasing the emitter energy difference. When $\Delta\omega_{12} < 2\mathrm{Im}(V_{12})$ or $\Delta\omega_{12} \sim 2\mathrm{Im}(V_{12})$ the emitters can strongly couple to each other, but when $\Delta\omega_{12} \gg 2\mathrm{Im}(V_{12})$, the emitters can be treated as independent emitters.

In addition to the peak separation, we also study the linewidth difference between the two reflection peaks as a function of emitter energy difference which is shown in Fig. 7(b). When $\Delta\omega_{12} = 0$, one reflection peak is a superradiant peak while the other one is a subradiant peak and their linewidth difference is about 2.1Γ which is close to the maximum value $2(\Gamma + \gamma)$. This means that when $\Delta\omega_{12} = 0$, the collective effect plays an important role. However, when $\Delta\omega_{12}$ is large, the linewidth difference between the two reflection peaks approach zero, which means that they behave like independent emitters. When $\Delta\omega_{12} = 2\mathrm{Im}(V_{12})$, the linewidth difference is about 66% of the maximum linewidth difference.

V. BEYOND TWO EMITTERS

Our theory shown in Sec. II can be extended to calculate the single-photon transport in a 1D waveguide coupled to an arbitrary number of emitters. In this section, we take five emitters as an example.

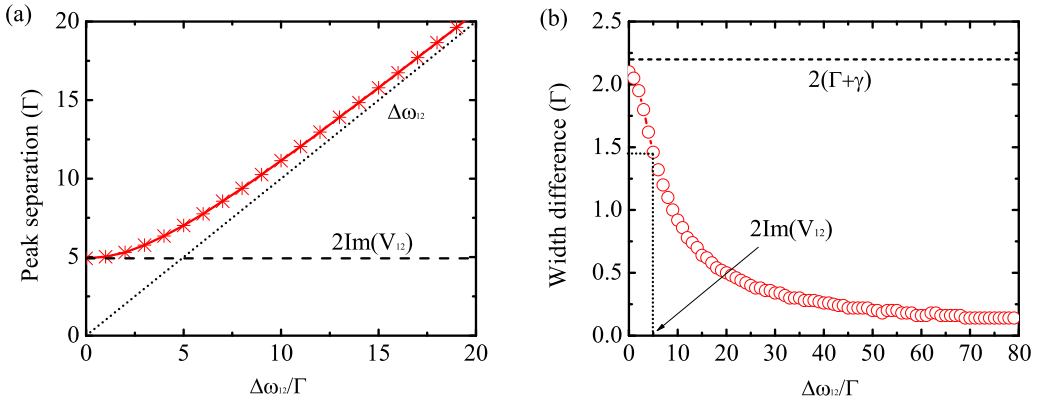

FIG. 7. Transition from coupled emitters to independent emitters. (a) The reflection peak separation as a function of emitter energy difference. (b) The linewidth difference between the two reflection peaks as a function of emitter energy difference. The parameters are as follows: $\gamma = 0.1\Gamma$ and $z_{12} = 0.05\lambda$.

In the first example, we assume that the emitters are identical and the emitter separation is 0.05λ. The emitter excitation dynamics and the emission spectra are shown in Figs. 8(a) and 8(b), respectively. Here, we assume a single-photon pulse with Gaussian shape is incident with $\Gamma_0 = 10\Gamma$ and when $\gamma = 0.2\Gamma$. From Fig. 8(a), we see that the emitters can exchange excitations rapidly and the coherent population oscillations can last for an extended period of time. Similar to the two-emitter case, the coherent population oscillation is due to the coherent part of the dipole-dipole interactions between the emitters. From Fig. 8(b) we can see that there are five reflection peaks with two superradiant peaks on the higher-frequency parts and three subradiant peaks on the lower-frequency parts. This indicates that the collective interactions between the emitters split the single-excitation states into five eigenstates with two superradiant states and

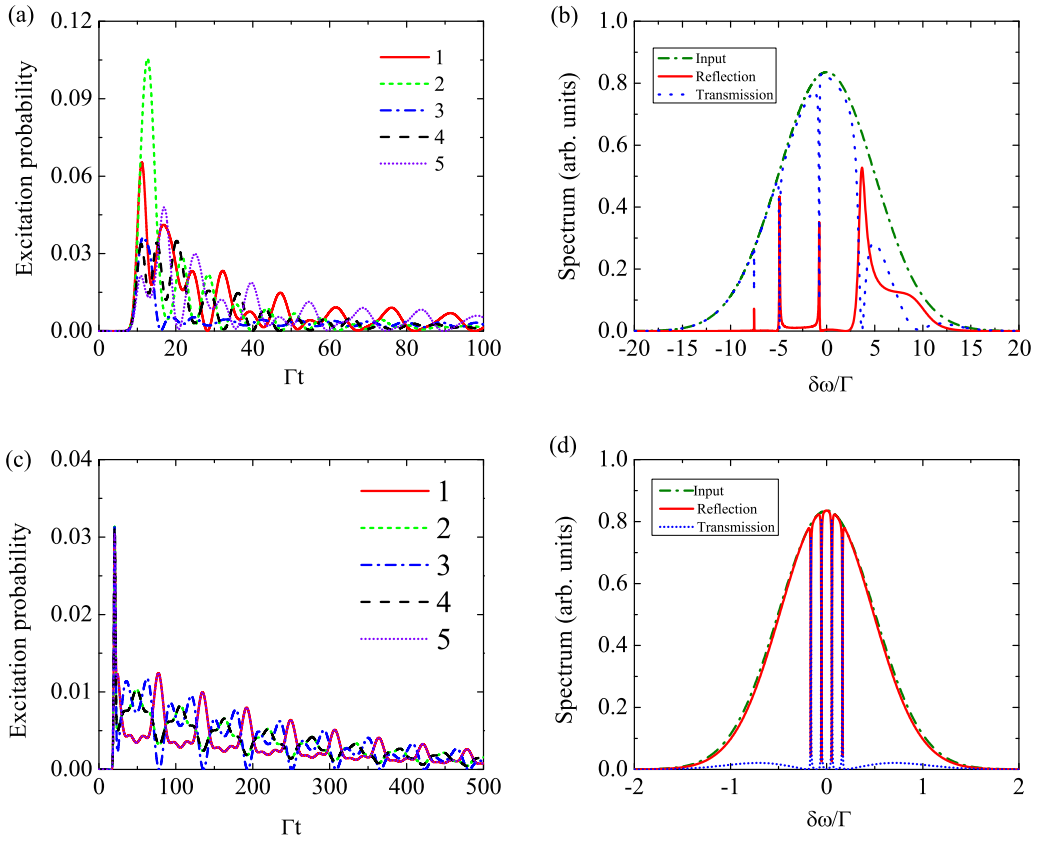

FIG. 8. (a), (c) Emitter excitation probabilities as a function of time where the red solid line is for emitter 1, the green short-dashed line is for emitter 2, the blue dash-dotted line is for emitter 3, the black dashed line is for emitter 4, and the violet short-dotted line is for emitter 5. (b), (d) Emission photon spectrum, where the green dash-dotted line is the input spectrum, the red solid line is the reflection spectrum, and the blue short-dotted line is the transmission spectrum. (a), (b) The emitters are identical with $z_{j,j+1} = 0.05\lambda$, $\gamma = 0.2\Gamma$, and $\Gamma_0 = 10\Gamma$. (c), (d) The emitters are nonidentical with $z_{j,j+1} = 0.5\lambda$, $\Delta\omega_{j,j+1} = 0.1\Gamma$, $\gamma = 0$, and $\Gamma_0 = 1\Gamma$.

three subradiant states. This may be used as a frequency filter which can filter out some special frequencies.

In the second example, we consider the case that the emitters are not identical. These emitters have a spatial separation 0.5λ and the neighboring emitters have an energy difference $\Delta\omega_{j,j+1} = 0.1\Gamma$. The emitter excitation dynamics and the emission spectra when $\gamma = 0$ are shown in Figs. 8(c) and 8(d) where we assume that the incident photon pulse has a Gaussian shape with $\Gamma_0 = \Gamma$. From Fig. 8(c), we see that the emitter excitations can oscillate and last for a very long time. The jth emitter and the $(N_a - j)$th emitter have almost the same excitation dynamics. The emission spectra are also very interesting. We can see that most of the photon spectra are reflected back but there are four very narrow transmission windows [Fig. 8(d)]. This is the generalization of the DIET shown in previous sections. This phenomena may be used to generate a single-photon frequency comb with very narrow linewidth [17].

VI. SUMMARY

In summary, we have developed dynamical equations and photon emission spectra for a single-photon transport in a 1D waveguide-QED system. In our generalized theory, the emitters can be either identical or nonidentical. In addition, the dipole-dipole interactions induced by both the waveguide and non-waveguide vacuum modes are included. This theory allows one to calculate the real-time evolution of the photon pulse and the emitters in a 1D waveguide-QED system and study the many-body physics.

We first compare the results with and without including the dipole-dipole interaction induced by the non-waveguide photon modes. The emitter dynamics and the scattering spectrum can be significantly modified by the dipole-dipole interaction induced by the non-waveguide vacuum modes if the emitter separation is much smaller than the resonance wavelength. We introduce a quantity (spectrum difference) to study the effects of the dipole-dipole interaction induced by the non-waveguide vacuum modes. We find that, when the emitter separation is much smaller than the resonant wavelength ($|V_{12}^{(nw)}| > \Gamma$), the dipole-dipole interaction induced by the non-waveguide photon modes can considerably influence the photon dynamics. When the emitter separation is of the order of or larger than the resonant wavelength ($|V_{12}^{(nw)}| \ll \Gamma$), the effects of the non-waveguide photon modes can be neglected.

We then studied the case of nonidentical emitters. The results show that, if the energy difference between the emitters is much larger than the energy shift due to the dipole-dipole interaction [$\Delta\omega_{12} \gg 2\mathrm{Im}(V_{12})$], the emitters behave like independent emitters. Otherwise, the emitters can strongly couple to each other. More interestingly, when the two emitters have close but nonzero energy difference, there is a very narrow transparency window around the resonance frequency due to the interference between the two collective decay channels. This is the demonstration of the dipole-dipole-induced electromagnetic transparency which may find important applications in quantum waveguide devices. For the case of multiple emitters, a single-photon frequency comb with very narrow comb linewidth can be generated.

ACKNOWLEDGMENT

This work is supported by a grant from the Qatar National Research Fund (QNRF) under NPRP project 7-210-1-032.

APPENDIX: DERIVATION OF EMITTER DYNAMICAL EQUATIONS

In this appendix, we derive the dynamical equations of the emitter system shown in Eq. (9). To derive Eq. (9), we need to calculate the second and third terms of Eq. (8).

For the second term of Eq. (8), the summation over k can be replaced by an integration

$$\sum_k \to \frac{L}{2\pi}\int_{-\infty}^{\infty} dk, \tag{A1}$$

where L is the quantization length in the propagation direction. The second term of Eq. (8) can then be calculated as

$$\sum_k g_k^j g_k^{l*} e^{ik(z_j-z_l)} e^{i\delta\omega_k^l t'} e^{-i\delta\omega_k^j t}$$

$$= \frac{L}{2\pi}\int_{-\infty}^{\infty} g_k^j g_k^{l*} e^{ik(z_j-z_l)} e^{i\delta\omega_k^l t'} e^{-i\delta\omega_k^j t} dk \tag{A2}$$

$$\simeq \frac{L}{2\pi} g_{k_a}^j g_{k_a}^{l*} e^{-i\Delta k_l v_g t'} e^{i\Delta k_j v_g t}\left[\int_0^{\infty} e^{ik(z_j-z_l)} e^{i(k-k_a)v_g(t'-t)} dk + \int_{-\infty}^{0} e^{ik(z_j-z_l)} e^{i(-k-k_a)v_g(t'-t)} dk\right] \tag{A3}$$

$$= \frac{L}{2\pi} g_{k_a}^j g_{k_a}^{l*} e^{-i\Delta k_l v_g t'} e^{i\Delta k_j v_g t}\left\{e^{ik_a(z_j-z_l)}\int_{-k_a}^{\infty} e^{i\delta k[(z_j-z_l)+v_g(t'-t)]} d\delta k + e^{-ik_a(z_j-z_l)}\int_{-k_a}^{\infty} e^{-i\delta k[(z_j-z_l)-v_g(t'-t)]} d\delta k\right\} \tag{A4}$$

$$\simeq \frac{L}{2\pi} g_{k_a}^j g_{k_a}^{l*} e^{-i\Delta k_l v_g t'} e^{i\Delta k_j v_g t}\left\{e^{ik_a(z_j-z_l)}\int_{-\infty}^{\infty} e^{i\delta k[(z_j-z_l)+v_g(t'-t)]} d\delta k + e^{-ik_a(z_j-z_l)}\int_{-\infty}^{\infty} e^{-i\delta k[(z_j-z_l)-v_g(t'-t)]} d\delta k\right\} \tag{A5}$$

$$= L g_{k_a}^j g_{k_a}^{l*} e^{-i\Delta k_l v_g t'} e^{i\Delta k_j v_g t}\{e^{ik_a(z_j-z_l)}\delta[(z_j-z_l)+v_g(t'-t)] + e^{-ik_a(z_j-z_l)}\delta[(z_j-z_l)-v_g(t'-t)]\} \tag{A6}$$

$$= \frac{L g_{k_a}^j g_{k_a}^{l*}}{v_g} e^{-i\Delta k_l v_g t'} e^{i\Delta k_j v_g t}\left\{e^{ik_a(z_j-z_l)}\delta\left[t' - \left(t - \frac{z_j-z_l}{v_g}\right)\right] + e^{-ik_a(z_j-z_l)}\delta\left[t' - \left(t + \frac{z_j-z_l}{v_g}\right)\right]\right\} \tag{A7}$$

$$= \frac{\Gamma_{jl}}{2} e^{-i\Delta k_l v_g t'} e^{i\Delta k_j v_g t} e^{ik_a|z_j - z_l|} \delta\left[t' - \left(t - \frac{|z_j - z_l|}{v_g}\right)\right] \tag{A8}$$

$$= \frac{\Gamma_{jl}}{2} e^{i\Delta\omega_{jl} t} e^{ik_l|z_{jl}|} \delta\left[t' - \left(t - \frac{|z_{jl}|}{v_g}\right)\right], \tag{A9}$$

where $\Delta\omega_{jl} = (k_j - k_l)v_g$ is the energy difference between two emitters, $\Delta k_j = k_j - k_a$, with k_a being a reference wave vector which can be chosen as the average wave vector (i.e., $k_a = \sum_j k_j/N_a$), and $\Gamma_{jl} = 2Lg^j_{k_a} g^{l*}_{k_a}/v_g$. From Eq. (A2) to Eq. (A3), we rewrite the integration into the left-propagation and right-propagation parts and assume that the coupling strength is uniform for the modes close to k_a. From Eq. (A4) to Eq. (A5), for $k_a \gg 0$ we can extend the lower bound of the integration from $-k_a$ to $-\infty$ and use the identity $\int_{-\infty}^{\infty} e^{ikx} dx = 2\pi\delta(x)$. In Eq. (A7), since $t' \leqslant t$, when $r_j > r_l$ only the second term survives. On the contrary, when $r_j < r_l$ only the first term survives. Therefore, Eq. (A7) can be rewritten as Eq. (A8). By inserting Eq. (A9) into the second term of Eq. (8) we can obtain

$$-\sum_{l=1}^{N} \frac{\Gamma_{jl}}{2} e^{i\Delta\omega_{jl} t} e^{ik_l|z_{jl}|} \alpha_l\left(t - \frac{|z_{jl}|}{v_g}\right), \tag{A10}$$

where $\Gamma_i = 2L|g^i_{k_a}|^2/v_g$ is the decay rate of the ith emitter due to the guided photon modes and $|z_{jl}| = |z_j - z_l|$ is the emitter separation along the waveguide direction.

To calculate the third term in Eq. (8), we first rewrite the summation over the wave vector $\vec{q}$ as an integration

$$\sum_{\vec{q}} = \frac{V}{(2\pi)^3} \int_0^{2\pi} d\phi \int_0^{\pi} \sin\theta d\theta \int_0^{\infty} q^2 dq, \tag{A11}$$

and the summation over the two polarizations as

$$\sum_{\lambda} g^j_{\vec{q},\lambda} g^{l*}_{\vec{q},\lambda} = \frac{\nu_q \mu^j_{ab} \mu^l_{ab}}{2\hbar\epsilon_0 V}\left[\left(\hat{\mu}_{ab} \cdot \hat{e}^1_{\vec{q}}\right)^2 + \left(\hat{\mu}_{ab} \cdot \hat{e}^2_{\vec{q}}\right)^2\right], \tag{A12}$$

where ν_q is the photon frequency with wave vector $\vec{q}$, μ_{ab} is the amplitude of the transition dipole moment with direction $\hat{\mu}_{ab}$, and $\hat{e}^1_{\vec{q}}$ and $\hat{e}^2_{\vec{q}}$ are the two polarization directions of the photon. Without loss of generality, we can assume the direction of the atomic transition dipole moment to be $\hat{\mu}_{ab} = (\sin\varphi, 0, \cos\varphi)$. The unit wave vector of the photon can be written as $\hat{q} = (\sin\theta\cos\phi, \sin\theta\sin\phi, \cos\theta)$ and the two polarization directions are given by $\hat{e}^1_{\vec{q}} = (\sin\phi, -\cos\phi, 0)$ and $\hat{e}^2_{\vec{q}} = (\cos\theta\cos\phi, \cos\theta\sin\phi, -\sin\theta)$. Thus, we have

$$\sum_{\lambda} g^j_{\vec{q},\lambda} g^{l*}_{\vec{q},\lambda} = \frac{\nu_q \mu^j_{ab} \mu^l_{ab}}{2\hbar\epsilon_0 V}[\sin^2\varphi\sin^2\phi + (\sin\varphi\cos\theta\cos\phi - \cos\varphi\sin\theta)^2]. \tag{A13}$$

For $j = l$, using the Weisskopf–Wigner approximation and $\int_{-\infty}^{\infty} d\nu_q e^{i(\nu_q - \omega)(t' - t)} = 2\pi\delta(t' - t)$, it is not difficult to obtain

$$\sum_{\vec{q},\lambda} \left|g^j_{\vec{q},\lambda}\right|^2 \int_0^t \alpha_j(t') e^{i\delta\omega^j_{\vec{q}} t'} dt' e^{-i\delta\omega^j_{\vec{q}} t} = \frac{\gamma_j}{2} \delta_{jl} \alpha_j(t), \tag{A14}$$

where $\gamma_j = k_a^3 \mu_j^2/3\pi\hbar\epsilon_0 V$ is the spontaneous decay rate of the jth atom due to the non-waveguide photon modes.

For $j \neq l$, by integrating out θ and ϕ, we have

$$\sum_{\vec{q},\lambda} g^j_{\vec{q},\lambda} g^{l*}_{\vec{q},\lambda} e^{-i\vec{q}\cdot(\vec{r}_j - \vec{r}_l)} = \frac{\nu_{k_a} \mu_j \mu_l}{4\pi^2\hbar\epsilon_0 V} \int_0^{\infty} q^2 \left\{\sin^2\varphi \frac{\sin(qr_{jl})}{qr_{jl}} + (1 - 3\cos^2\varphi)\left[\frac{\cos(qr_{jl})}{(qr_{jl})^2} - \frac{\sin(qr_{jl})}{(qr_{jl})^3}\right]\right\} dq. \tag{A15}$$

where we assume that only a narrow band of frequency around resonant frequency can couple to the system, i.e., $\nu_q \simeq \nu_{k_a}$. We then have

$$\sum_{\vec{q},\lambda} g^j_{\vec{q},\lambda} g^{l*}_{\vec{q},\lambda} e^{-i\vec{q}\cdot(\vec{r}_j - \vec{r}_l)} e^{i\delta\omega^{jl}_q (t' - t)}$$

$$= \frac{\nu_{k_a} \mu_j \mu_l}{4\pi^2\hbar\epsilon_0 V} e^{-i\Delta k_l v_g t'} e^{i\Delta k_j v_g t} \int_0^{\infty} q^2 \left\{\sin^2\varphi \frac{\sin(qr_{jl})}{qr_{jl}} + (1 - 3\cos^2\varphi)\left[\frac{\cos(qr_{jl})}{(qr_{jl})^2} - \frac{\sin(qr_{jl})}{(qr_{jl})^3}\right]\right\} e^{i(q - k_a)v_g(t' - t)} dq. \tag{A16}$$

The integration over the first term in the curly bracket can be calculated as follows:

$$\int_0^\infty q^2 \frac{\sin(qr_{jl})}{qr_{jl}} e^{i(q-k_a)v_g(t'-t)} dq = \frac{1}{2ir_{jl}} \int_0^\infty q(e^{iqr_{jl}} - e^{-iqr_{jl}}) e^{i(q-k_a)v_g(t'-t)} dq \tag{A17}$$

$$\simeq \frac{k_a}{2ir_{jl}} \left[\int_{-k_a}^\infty e^{ik_a r_{jl}} e^{i\delta q[r_{jl}+v_g(t'-t)]} d\delta q - \int_{-k_a}^\infty e^{-ik_a r_{jl}} e^{i\delta q[r_{jl}-v_g(t'-t)]} d\delta q \right] \tag{A18}$$

$$\simeq \frac{k_a}{2ir_{jl}} \left[\int_{-\infty}^\infty e^{ik_a r_{jl}} e^{i\delta[r_{jl}+v_g(t'-t)]} d\delta q - \int_{-\infty}^\infty e^{-ik_a r_{jl}} e^{i\delta q[r_{jl}-v_g(t'-t)]} d\delta q \right] \tag{A19}$$

$$= \frac{2\pi k_a}{2ir_{jl}v_g} \left\{ e^{ik_a r_{jl}} \delta\left[t' - \left(t - \frac{r_{jl}}{v_g} \right) \right] - e^{-ik_a r_{jl}} \delta\left[t' - \left(t + \frac{r_{jl}}{v_g} \right) \right] \right\} \tag{A20}$$

$$= \frac{\pi k_a^2}{v_g} \frac{1}{ik_a r_{jl}} e^{ik_a|r_{jl}|} \delta\left[t' - \left(t - \frac{|r_{jl}|}{v_g} \right) \right]. \tag{A21}$$

According to the Weisskopf–Wigner approximation [66], since the phase varies little around the resonant frequency and has the major contribution, from Eqs. (A17) to (A18), we use $q \simeq k_a$ and move q out of the integration, and change the lower bound of the integration from $-k_a$ to $-\infty$ from Eq. (A18) to Eq. (A19). Similarly, we have the second term and the third term of Eq. (A15), which are respectively given by

$$\int_0^\infty q^2 \frac{\cos(qr_{jl})}{(qr_{jl})^2} e^{i(q-k_a)v_g(t'-t)} dq = \frac{\pi k_a^2}{v_g} \frac{1}{(k_a r_{jl})^2} e^{ik_a|r_{jl}|} \delta\left[t' - \left(t - \frac{|r_{jl}|}{v_g} \right) \right], \tag{A22}$$

and

$$\int_0^\infty q^2 \frac{\sin(qr_{jl})}{(qr_{jl})^3} e^{i(q-k_a)v_g(t'-t)} dq = \frac{\pi k_a^2}{v_g} \frac{1}{i(k_a r_{jl})^3} e^{ik_a|r_{jl}|} \delta\left[t' - \left(t - \frac{|r_{jl}|}{v_g} \right) \right]. \tag{A23}$$

Upon inserting Eqs. (A21)–(A23) into Eq. (A15), we have

$$\sum_{\vec{q},\lambda} g_{\vec{q},\lambda}^j g_{\vec{q},\lambda}^{l*} e^{-i\vec{q}\cdot(\vec{r}_j - \vec{r}_l)} e^{i\delta\omega_q^l t'} e^{-i\delta\omega_q^j t}$$

$$= \frac{3\gamma_{jl}}{4} e^{-i\Delta k_l v_g t'} e^{i\Delta k_j v_g t} \left\{ \sin^2\varphi \frac{-i}{k_a r_{jl}} + (1 - 3\cos^2\varphi) \left[\frac{1}{(k_a r_{jl})^2} + \frac{i}{(k_a r_{jl})^3} \right] \right\} e^{ik_a|r_{jl}|} \delta\left[t' - \left(t - \frac{|r_{jl}|}{v_g} \right) \right] \tag{A24}$$

$$= \frac{3\gamma_{jl}}{4} e^{-i\Delta\omega_{jl} t} e^{ik_l|r_{jl}|} \left\{ \sin^2\varphi \frac{-i}{k_a r_{jl}} + (1 - 3\cos^2\varphi) \left[\frac{1}{(k_a r_{jl})^2} + \frac{i}{(k_a r_{jl})^3} \right] \right\} \delta\left[t' - \left(t - \frac{|r_{jl}|}{v_g} \right) \right]. \tag{A25}$$

Upon inserting Eqs. (A10) and (A25) into Eq. (8) we can obtain the dynamical equations of the emitters

$$\dot{\alpha}_j(t) = b_j(t) - \sum_{l=1}^N \left[V_{jl}^{(w)} e^{ik_l|z_{jl}|} \alpha_l\left(t - \frac{|z_{jl}|}{v_g} \right) + V_{jl}^{(nw)} e^{ik_l|r_{jl}|} \alpha_l\left(t - \frac{|r_{jl}|}{v_g} \right) \right] e^{i\Delta\omega_{jl} t}, \tag{A26}$$

where

$$b_j(t) = -\frac{i}{2\pi} \sqrt{\frac{\Gamma v_g L}{2}} e^{ik_a z_j} e^{i\Delta k_j v_g t} \int_{-\infty}^\infty \beta_{\delta k}(0) e^{i\delta k(r_j - v_g t)} d\delta k, \tag{A27}$$

$V_{jj}^{(w)} = \Gamma_j/2$ and $V_{jj}^{(nw)} = \gamma_j/2$. For $j \neq l$, $V_{jl}^{(w)} = \sqrt{\Gamma_j \Gamma_l}/2$ is the dipole-dipole coupling due to the waveguide modes and

$$V_{jl}^{(nw)} = \frac{3\sqrt{\gamma_j \gamma_l}}{4} \left[\sin^2\varphi \frac{-i}{k_a r_{jl}} + (1 - 3\cos^2\varphi) \frac{1}{(k_a r_{jl})^2} + \frac{i}{(k_a r_{jl})^3} \right] \tag{A28}$$

is the dipole-dipole interaction due to the non-waveguide photon modes. The term $e^{-i\Delta\omega_{jl} t}$ is due to the energy difference between the two emitters. If the two emitters are the same, this term becomes unity and the equation returns back to the case for identical emitters.

[1] S. Noda, M. Fujita, and T. Asano, Spontaneous-emission control by photonic crystals and nanocavities, Nature (London) **1**, 449 (2007).

[2] M. D. Leistikow, A. P. Mosk, E. Yeganegi, S. R. Huisman, A. Lagendijk, and W. L. Vos, Inhibited Spontaneous Emission of Quantum Dots Observed in a 3D Photonic Band Gap, Phys. Rev. Lett. **107**, 193903 (2011).

[3] B. Dayan, A. S. Parkins, T. Aoki, E. P. Ostby, K. J. Vahala, and H. J. Kimble, A photon turnstile dynamically regulated by one atom, Science **319**, 1062 (2013).

[4] D. Englund, A. Faraon, B. Zhang, Y. Yamamoto, and J. Vučković, Generation and transfer of single photons on a photonic crystal chip, Opt. Express **15**, 5550 (2007).

[5] A. V. Akimov, A. Mukherjee, C. L. Yu, D. E. Chang, A. S. Zibrov, P. R. Hemmer, H. Park, and M. D. Lukin, Generation of single optical plasmons in metallic nanowires coupled to quantum dots, Nature (London) **450**, 402 (2007).

[6] A. Wallraff, D. I. Schuster, A. Blais, L. Frunzio, R.-S. Huang, J. Majer, S. Kumar, S. M. Girvin, and R. J. Schoelkopf, Strong coupling of a single photon to a superconducting qubit using circuit quantum electrodynamics, Nature (London) **431**, 162 (2004).

[7] A. A. Abdumalikov, Jr., O. Astafiev, A. M. Zagoskin, Y. A. Pashkin, Y. Nakamura, and J. S. Tsai, Electromagnetically Induced Transparency on a Single Artificial Atom, Phys. Rev. Lett. **104**, 193601 (2010).

[8] I.-C. Hoi, C. M. Wilson, G. Johansson, T. Palomaki, B. Peropadre, and P. Delsing, Demonstration of a Single-Photon Router in the Microwave Regime, Phys. Rev. Lett. **107**, 073601 (2011).

[9] I.-C. Hoi, T. Palomaki, J. Lindkvist, G. Johansson, P. Delsing, and C. M. Wilson, Generation of Nonclassical Microwave States using an Artificial Atom in 1D Open Space, Phys. Rev. Lett. **108**, 263601 (2012).

[10] A. F. van Loo, A. Fedorov, K. Lalumiére, B. C. Sanders, A. Blais, and A. Wallraff, Photon-mediated interactions between distant artificial atoms, Science **342**, 1494 (2013).

[11] J. S. Douglas, H. Habibian, C.-L. Hung, A. V. Gorshkov, H. J. Kimble, and D. E. Chang, Quantum many-body models with cold atoms coupled to photonic crystals, Nat. Photonics **9**, 326 (2015).

[12] J.-T. Shen and S. Fan, Strongly Correlated Two-Photon Transport in a One-Dimensional Waveguide Coupled to a Two-Level System, Phys. Rev. Lett. **98**, 153003 (2007).

[13] H. Zheng, D. J. Gauthier, and H. U. Baranger, Cavity-Free Photon Blockade Induced by Many-Body Bound States, Phys. Rev. Lett. **107**, 223601 (2011).

[14] D. Roy, Two-Photon Scattering by a Driven Three-Level Emitter in a One-Dimensional Waveguide and Electromagnetically Induced Transparency, Phys. Rev. Lett. **106**, 053601 (2011).

[15] T. Shi, S. Fan, and C. P. Sun, Two-photon transport in a waveguide coupled to a cavity in a two-level system, Phys. Rev. A **84**, 063803 (2011).

[16] Yao-L. L. Fang, and H. U. Baranger, Waveguide QED: Power spectra and correlations of two photons scattered off multiple distant qubits and a mirror, Phys. Rev. A **91**, 053845 (2015).

[17] Z. Liao, X. Zeng, H. Nha, and M. S. Zubairy, Photon transport in a one-dimensional nanophotonic waveguide QED system, Phys. Scr. **91**, 063004 (2016).

[18] J.-T. Shen and S. Fan, Coherent photon transport from spontaneous emission in one-dimensional waveguides, Opt. Lett. **30**, 2001 (2005).

[19] J.-T. Shen and S. Fan, Coherent Single Photon Transport in a One-Dimensional Waveguide Coupled with Superconducting Quantum Bits, Phys. Rev. Lett. **95**, 213001 (2005).

[20] V. I. Yudson and P. Reineker, Multiphoton scattering in a one-dimensional waveguide with resonant atoms, Phys. Rev. A **78**, 052713 (2008).

[21] T. S. Tsoi and C. K. Law, Quantum interference effects of a single photon interacting with an atomic chain inside a one-dimensional waveguide, Phys. Rev. A **78**, 063832 (2008).

[22] H. Zheng, D. J. Gauthier, and H. U. Baranger, Waveguide QED: Many-body bound-state effects in coherent and Fock-state scattering from a two-level system, Phys. Rev. A **82**, 063816 (2010).

[23] M.-T. Cheng, X.-S. Ma, M.-T. Ding, Y.-Q. Luo, and G.-X. Zhao, Single-photon transport in one-dimensional coupled-resonator waveguide with local and nonlocal coupling to a nanocavity containing a two-level system, Phys. Rev. A **85**, 053840 (2012).

[24] J. F. Huang, T. Shi, C. P. Sun, and F. Nori, Controlling single-photon transport in waveguides with finite cross section, Phys. Rev. A **88**, 013836 (2013).

[25] Q. Li, L. Zhou, and C. P. Sun, Waveguide quantum electrodynamics: Controllable channel from quantum interference, Phys. Rev. A **89**, 063810 (2014).

[26] S. Fan, S. E. Kocabas, and J.-T. Shen, Input-output formalism for few-photon transport in one-dimensional nanophotonic waveguides coupled to a qubit, Phys. Rev. A **82**, 063821 (2010).

[27] K. Lalumière, B. C. Sanders, A. F. van Loo, A. Fedorov, A. Wallraff, and A. Blais, Input-output theory for waveguide QED with an ensemble of inhomogeneous atoms, Phys. Rev. A **88**, 043806 (2013).

[28] S. Xu and S. Fan, Input-output formalism for few-photon transport: A systematic treatment beyond two photons, Phys. Rev. A **91**, 043845 (2015).

[29] T. Shi and C. P. Sun, Lehmann–Symanzik–Zimmermann reduction approach to multiphoton scattering in coupled-resonator arrays, Phys. Rev. B **79**, 205111 (2009).

[30] M. Pletyukhov and V. Gritsev, Scattering of massless particles in one-dimensional chiral channel, New J. Phys. **14**, 095028 (2012).

[31] A. Roulet and V. Scarani, Solving the scattering of N photons on a two-level atom without computation, New J. Phys. **18**, 093035 (2016).

[32] E. Rephaeli, J.-T. Shen, and S. Fan, Full inversion of a two-level atom with a single-photon pulse in one-dimensional geometries, Phys. Rev. A **82**, 033804 (2010).

[33] Y. Chen, M. Wubs, J. Mørk, and A. F. Koenderink, Coherent single-photon absorption by single emitters coupled to one-dimensional nanophotonic waveguides, New J. Phys. **13**, 103010 (2011).

[34] Z. Liao, X. Zeng, S.-Y. Zhu, and M. S. Zubairy, Single-photon transport through an atomic chain coupled to a one-dimensional nanophotonic waveguide, Phys. Rev. A **92**, 023806 (2015).

[35] B. Q. Baragiola, R. L. Cook, A. M. Brańczyk, and J. Combes, N-photon wave packets interacting with an arbitrary quantum system, Phys. Rev. A **86**, 013811 (2012).

[36] T. Shi, D. E. Chang, and J. I. Cirac, Multiphoton-scattering theory and generalized master equations, Phys. Rev. A **92**, 053834 (2015).

[37] L. Zhou, H. Dong, Y.-X. Liu, C. P. Sun, and F. Nori, Quantum supercavity with atomic mirrors, Phys. Rev. A **78**, 063827 (2008).

[38] D. E. Chang, L. Jiang, A. V. Gorshkov, and H. J. Kimble, Cavity QED with atomic mirrors, New J. Phys. **14**, 063003 (2012).

[39] P.-O. Guimond, A. Roulet, H. N. Le, and V. Scarani, Rectification of light in the quantum regime, Phys. Rev. A **93**, 023808 (2016).
[40] V. M. Menon, W. Tong, F. Xia, C. Li, and S. R. Forrest, Nonreciprocity of counterpropagating signals in a monolithically integrated Sagnac interferometer, Opt. Lett. **29**, 513 (2004).
[41] Y. Shen, M. Bradford, and J.-T. Shen, Single-Photon Diode by Exploiting the Photon Polarization in a Waveguide, Phys. Rev. Lett. **107**, 173902 (2011).
[42] J. Dai, A. Roulet, H. N. Le, and V. Scarani, Rectification of light in the quantum regime, Phys. Rev. A **92**, 063848 (2015).
[43] M. Bradford, K. C. Obi, and J.-T. Shen, Efficient Single-Photon Frequency Conversion using a Sagnac Interferometer, Phys. Rev. Lett. **108**, 103902 (2012).
[44] M. Bradford and J.-T. Shen, Single-photon frequency conversion by exploiting quantum interference, Phys. Rev. A **85**, 043814 (2012).
[45] W.-B. Yan, J.-F. Huang, and H. Fan, Tunable single-photon frequency conversion in a Sagnac interferometer, Sci. Rep. **3**, 3555 (2013).
[46] Z. H. Wang, L. Zhou, Y. Li, and C. P. Sun, Controllable single-photon frequency converter via a one-dimensional waveguide, Phys. Rev. A **89**, 053813 (2014).
[47] D. E. Chang, A. S. Sørensen, E. A. Demler, and M. D. Lukin, A single-photon transistor using nanoscale surface plasmons, Nat. Phys. **3**, 807 (2007).
[48] D. Witthaut and A. S. Sorensen, Photon scattering by a three-level emitter in a one-dimensional waveguide, New J. Phys. **12**, 043052 (2010).
[49] T. G. Tiecke, J. D. Thompson, N. P. de Leon, L. R. Liu, V. Vuletić, and M. D. Lukin, Nanophotonic quantum phase switch with a single atom, Nature (London) **508**, 241 (2014).
[50] A. Javadi, I. Söllner, M. Arcari, S. L. Hansen, L. Midolo, S. Mahmoodian, G. Kirsanske, T. Pregnolato, E. H. Lee, J. D. Song, S. Stobbe, and P. Lodahl, Single-photon non-linear optics with a quantum dot in a waveguide, Nat. Commun. **6**, 8655 (2015).
[51] W.-B. Yan and H. Fan, Single-photon quantum router with multiple output ports, Sci. Rep. **4**, 4820 (2014).
[52] F. Ciccarello, D. E. Browne, L. C. Kwek, H. Schomerus, M. Zarcone, and S. Bose, Quasideterministic realization of a universal quantum gate in a single scattering process, Phys. Rev. A **85**, 050305(R) (2012).
[53] H. Zheng, D. J. Gauthier, and H. U. Baranger, Waveguide-QED-Based Photonic Quantum Computation, Phys. Rev. Lett. **111**, 090502 (2013).
[54] V. Paulisch, H. J. Kimble, and A. Gonzalez-Tudela, Universal quantum computation in waveguide QED using decoherence free subspaces, New J. Phys. **18**, 043041 (2016).
[55] Z. Liao, H. Nha, and M. S. Zubairy, Single-photon frequency-comb generation in a one-dimensional waveguide coupled to two atomic arrays, Phys. Rev. A **93**, 033851 (2016).
[56] E. Vetsch, D. Reitz, G. Sagué, R. Schmidt, S. T. Dawkins, and A. Rauschenbeutel, Optical Interface Created by Laser-Cooled Atoms Trapped in the Evanescent Field Surrounding an Optical Nanofiber, Phys. Rev. Lett. **104**, 203603 (2010).
[57] C.-L. Hung, S. M. Meenehan, D. E. Chang, O. Painter, and H. J. Kimble, Trapped atoms in one-dimensional photonic crystals, New J. Phys. **15**, 083026 (2013).
[58] A. Gonzalez-Tudela, C.-L. Hung, D. E. Chang, J. I. Cirac, and H. J. Kimble, Subwavelength vacuum lattices and atom–atom interactions in two-dimensional photonic crystals, Nat. Photonics **9**, 320 (2015).
[59] C.-J. Wang, L. Huang, B. A. Parviz, and L. Y. Lin, Subdiffraction photon guidance by quantum-dot cascades, Nano Lett. **6**, 2549 (2006).
[60] R. H. Dicke, Coherence in spontaneous radiation processes, Phys. Rev. **93**, 99 (1954).
[61] Z. Ficek and S. Swain, *Quantum Interference and Quantum Coherence: Theory and Experiment* (Springer, New York, 2004).
[62] Z. Liao, M. Al-Amri, and M. S. Zubairy, Resonance-fluorescence-localization microscopy with subwavelength resolution, Phys. Rev. A **85**, 023810 (2012).
[63] Z. Liao and M. S. Zubairy, Single-photon modulation by the collective emission of an atomic chain, Phys. Rev. A **90**, 053805 (2014).
[64] H. Kim, D. Sridharan, T. C. Shen, G. S. Solomon, and E. Waks, Strong coupling between two quantum dots and a photonic crystal cavity using magnetic field tuning, Opt. Express **19**, 2589 (2011).
[65] R. Puthumpally-Joseph, M. Sukharev, O. Atabek, and E. Charron, Dipole-Induced Electromagnetic Transparency, Phys. Rev. Lett. **113**, 163603 (2014).
[66] M. O. Scully and M. S. Zubairy, *Quantum Optics* (Cambridge University Press, Cambridge, 2001).
[67] J.-T. Shen and S. Fan, Theory of single-photon transport in a single-mode waveguide. I. Coupling to a cavity containing a two-level atom, Phys. Rev. A **79**, 023837 (2009).
[68] U. Fano, Effects of configuration interaction on intensities and phase shifts, Phys. Rev. **124**, 1866 (1961).
[69] M.-T. Cheng and Y.-Y. Song, Fano resonance analysis in a pair of semiconductor quantum dots coupling to a metal nanowire, Opt. Lett. **837**, 978 (2012).
[70] S. E. Harris, J. E. Field, and A. Imamoğlu, Nonlinear Optical Processes using Electromagnetically Induced Transparency, Phys. Rev. Lett. **64**, 1107 (1990).